AIAA 95-3943

Interactive Flutter Analysis and Parametric Study for Conceptual Wing Design

Vivek Mukhopadhyay
Systems Analysis Branch
Aeronautical Systems Analysis Division
MS 248, NASA Langley Research Center
Hampton, Virginia 23681-0001

1st AIAA Aircraft Engineering, Technology and Operations Congress
September 19-21, 1995
Los Angeles, California

INTERACTIVE FLUTTER ANALYSIS AND PARAMETRIC STUDY FOR CONCEPTUAL WING DESIGN

Vivek Mukhopadhyay*
Systems Analysis Branch,
Aeronautical Systems Analysis Division
MS 248, NASA Langley Research Center

Abstract

An interactive computer program was developed for wing flutter analysis in the conceptual design stage. The objective was to estimate the flutter instability boundary of a flexible cantilever wing, when well defined structural and aerodynamic data are not available, and then study the effect of change in Mach number, dynamic pressure, torsional frequency, sweep, mass ratio, aspect ratio, taper ratio, center of gravity, and pitch inertia, to guide the development of the concept. The software was developed on MathCad** platform for Macintosh, with integrated documentation, graphics, database and symbolic mathematics. The analysis method was based on non-dimensional parametric plots of two primary flutter parameters, namely Regier number and Flutter number, with normalization factors based on torsional stiffness, sweep, mass ratio, aspect ratio, center of gravity location and pitch inertia radius of gyration. The plots were compiled in a Vaught Corporation report from a vast database of past experiments and wind tunnel tests. The computer program was utilized for flutter analysis of the outer wing of a Blended Wing Body concept, proposed by McDonnell Douglas Corporation. Using a set of assumed data, preliminary flutter boundary and flutter dynamic pressure variation with altitude, Mach number and torsional stiffness were determined.

1. Introduction

During the conceptual design stage, it is often necessary to obtain initial estimates of flutter instability boundary, when only the basic planform of the wing is known, and much of the structural, mass and inertia properties are yet to be established. It is also very useful to conduct a parametric study to determine the effect of change in Mach number, dynamic pressure, torsional frequency, wing sweepback angle, mass ratio, aspect ratio, taper ratio, center of gravity, and pitch moment of inertia, on flutter instability boundary. In order to meet these objectives, an interactive computer program was developed for preliminary flutter analysis of a flexible cantilever wing. The computer program runs on a MathCad[1] platform for Macintosh, which has integrated documentation, graphics, database and symbolic mathematics. The current flutter analysis method is based on an experimental database and non-dimensional parametric plots of two primary flutter parameters, namely Regier number and Flutter number, and their variation with Mach number, dynamic pressure, with normalization factors based on geometry, torsional stiffness, sweep, mass ratio, aspect ratio, center of gravity position, pitch inertia radius of gyration, etc. The analysis database and parametric plots were compiled in a handbook by Harris[2] from a large number of wind-tunnel flutter model test data. The Regier number is a stiffness-altitude parameter, first studied by Regier[3] for scaled dynamic flutter models. An extension to the use of the Regier number as a flutter design parameter was presented by Frueh[4]. In a recent paper by Dunn[5], Regier number was used to impose flutter constraints on the structural design and optimization of an ideal wing.

The analysis method was utilized to estimate the flutter boundary and stiffness requirements of the outer wing of a Blended-Wing-Body (BWB) concept, proposed by Liebeck et. al.[6] at McDonnell Douglas Corporation under NASA contract NAS1-18763. Preliminary flutter boundary and flutter dynamic pressure variation with altitude, Mach number, and root-chord torsional stiffness, using a set of initial data were determined.

2. Nomenclature

AR	aspect ratio based on half wing
a	speed of sound
a_eq	equivalent airspeed = $a/\sqrt{\sigma}$
a0	speed of sound at sea level
C_75	wing chord at 75% semispan
C	chord at 60% semispan
cg	center of gravity
CGR	center of gravity ratio
CR	root chord
CT	tip chord

* Associate Fellow, AIAA
**MathCad is registered Trademark of MathSoft Inc.

EI section bending stiffness (lb-ft^2)
F Flutter number = M / R
F_ normalized Flutter number
g acceleration due to gravity
GJ_root root-chord torsional stiffness (lb-ft^2)
Ka torsional frequency factor
K_all total correction factor
K_Ar aspect ratio correction factor
K_cg center of gravity correction factor
K_flex root flexibility correction
K_λ taper ratio correction factor
K_μ mass ratio correction factor
K_Rgyb radius of gyration ratio factor
I_60 wing pitch inertia at 60% span (lb-ft^2)
L effective beam length
M Mach number
MAC mean aerodynamic chord
MGC mean geometric chord
q dynamic pressure
R Surface Regier number
R Regier number
R_ normalized Regier number
R_{gyb} radius of gyration ratio
V flight velocity
V_eq equivalent flight velocity = $V\sqrt{\sigma}$
V_R Regier surface velocity index
W_tot weight of wing per side (lb)
Λ wing sweep back angle
λ wing taper ratio
μ wing mass ratio
μ0 mass ratio at sea level
ρ air density
ρ0 air density at sea level
σ air density ratio ρ/ρ0
ω_α wing torsional frequency
ω_h wing bending frequency

Symbol subscript extensions
_avr average plot
_env envelope plot
_eq equivalent air speed
_KT velocity in Knots
_ms medium sweep

3. General Assumptions

Figure 1 defines the conventional straight leading and trailing edge wing planform for which the current analysis is valid. The primary input data required are root-chord CR, tip-chord CT, effective semispan, sweep at quarter chord Λ, running pitch moment of inertia I_60 and running weight at 60% effective semispan W_60, total weight of the exposed surface W_tot, reference flight altitude and Mach number. The altitude and Mach number are generally chosen at sea level and at design dive speed, respectively.

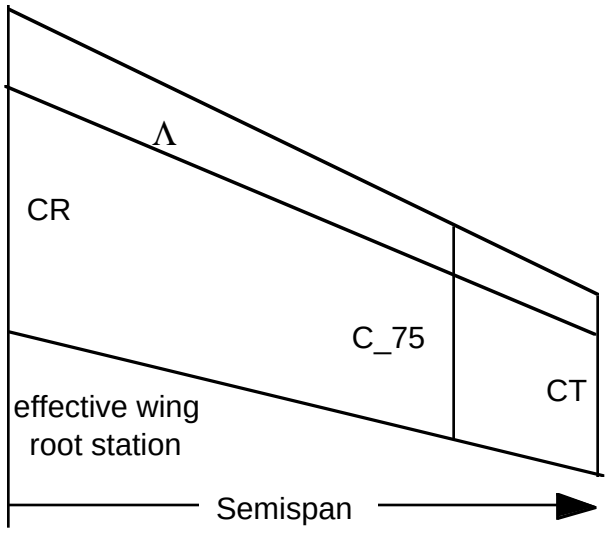

Figure 1. Conventional wing planform geometry definition for flutter analysis.

The wing is assumed to be a cantilever beam clamped at an effective root station, from where the outer wing acts like a lifting surface with bending and torsional flexibility. Later this effective root is considered to be restrained with a soft spring to account for the effect of bending and torsional flexibility at this point. This feature is useful for an all moving surface mounted on a flexible rod or for a blended wing-body type structure where the outer flexible wing primarily contributes to flutter and the inner part is practically rigid, but the effective root station of the flexible outer wing has some bending freedom.

The interactive analysis starts with specifying the geometric data and the critical design input parameters. These numerical data are assigned or changed interactively on the computer screen, for all the parameters which are followed by the assignment symbol :=, and are marked as INPUT. At a later stage, for parametric study, a series of values can also be assigned directly. The rest of the analysis equations, related data and functions are automatically calculated, and all data are plotted to reflect the effect of the new input parameters. The units are also checked for compatibility before calculations are performed. A typical interactive data input screen is shown in figure 2 for root and midwing torsional stiffness, Mach number, altitude, sweepback angle at reference chord fraction, running mass moment of inertia, running weight at 60% semispan and pitch moment of inertia. The effective beam length is calculated from the effective semispan and sweep angle. The input data is used to compute the torsion frequency and two basic flutter indexes, namely Regier number and Flutter number which are described next.

INPUT Root and Tip chord: $CR := 35.4 \cdot ft$ $CT := 14.5 \cdot ft$ $\lambda := \frac{CT}{CR}$

INPUT effective SEMISPAN: $Semi\_span := 106.8 \cdot ft$ $\lambda = 0.41$

DefineEffective Aspect ratio: (ONE SIDE ONLY) $AR := \frac{Semi\_span}{0.5 \cdot (CR + CT)}$ $AR = 4.281$

INPUT Mean Aerodynamic chord: $MAC := 33.75 \cdot ft$

INPUT Tosional Stiffness at effective root, GJ_root and midspan, along and normal to elastic axis:

$GJ\_root := 40 \cdot 10^8 \cdot lb \cdot ft^2$ $GJ\_mid := 24 \cdot 10^8 \cdot lb \cdot ft^2$ $GJ\_Ratio := \frac{GJ\_mid}{GJ\_root}$

INPUT Flight Profile, Mach and Altitude in 1000 ft: $Mach := 0.6$ $Alt := 0$

INPUT WEIGHT DATA:

INPUT Running Mass moment of inertia at 60% exposed Span, in weight unit: $I\_60 := 16000 \cdot \left(\frac{lb \cdot ft^2}{ft}\right)$

Pitch axis moment of inertia I_pitch $I\_pitch := 7.0 \cdot 10^5 \cdot lb \cdot ft^2$

Running weight at 60% of exposed Span station W_60 $W\_60 := 500 \cdot \frac{lb}{ft}$

Figure 2 A typical interactive screen for INPUT stiffness, Mach number, altitude and weight data.

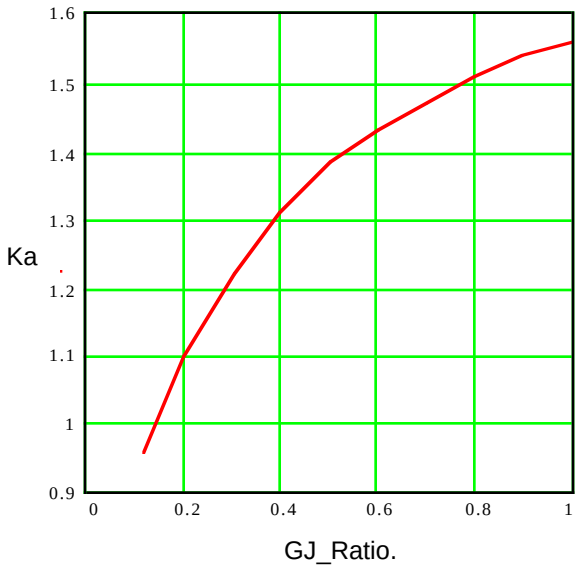

Figure 3. Interpolated plot of factor Ka as a function of GJ_Ratio for estimating torsional frequency.

4. Regier number and Flutter number

The first step in the analysis process is to compute the all important nondimensional surface Regier number R and Regier surface velocity index V_R of the wing, which are defined at sea level as

$$\text{Regier\_no } R := V\_R / a0 \qquad (1)$$

$$V\_R = 0.5 C\_75 \omega_\alpha \sqrt{\mu 0} \qquad (2)$$

For analysis purposes, V_R is also defined as a function denoted by v_R(GJ_Ratio, GJ_root, I_60, L, b_75, μ0). Although V_R is actually a stiffness parameter proportional to the wing uncoupled torsional frequency ω_α, it will be referred to as Regier surface velocity index in this paper, since it has the unit of velocity. During the conceptual design stage, detailed structural data are generally not available for computing the wing uncoupled torsional frequency ω_α, hence an empirical formula[2] based on a torsional frequency factor Ka is used, as shown in Eq.(3) in radians/second unit.

$$\omega_\alpha = Ka \sqrt{\frac{GJ\_root}{I\_60 / g}} \qquad (3)$$

Figure 3 shows the plot of the factor Ka as a function of GJ_Ratio, which is defined by torsional stiffness GJ at midwing divided by GJ_root. The original plot

was compiled[2] by computing Ka from numerous experimental data and then drawing a mean line through the data. Using the computed GJ_Ratio, the factor Ka is automatically calculated from figure 3 using an interpolation function, and is then used to compute the torsional frequency ω_α from Eq.(3). If a detailed finite element model of the wing is available for vibration frequency analysis, a better estimate of the torsional frequency ω_α can be used instead.

The second important non dimensional parameter called Flutter number F is defined as equivalent air speed at sea level V_eq divided by Regier surface velocity index *V_R* as shown in Eq.(4). Note that Regier number *R* and Flutter number F are inversely proportional and satisfy Eq.(5). The Flutter number corresponding to the equivalent flutter velocity is determined from a set of non dimensional plots as described next and is compared with the actual flutter number in order to determine the flutter velocity safety margin, which should be above 20% at sea level maximum dive speed.

Flutter_no F := V_eq / *V_R* (4)

Flutter_no F := M / Regier_no (5)

5. Flutter Boundary Estimation

The basic flutter analysis process and experimental data plots compiled by Harris[2] are briefly summarized in this section and in the appendix. Only those plots which are applicable to a conventional straight leading and trailing edge planform wing with moderate sweep between 20 and 40 degrees, are presented here. The flutter analysis is accomplished using two basic plots of Regier number and Flutter number versus Mach number shown in figures 4 and 5. These plots were based on experimental and analytical flutter studies of these two flutter indexes which were normalized by certain values of eight basic parameters, namely mass ratio, sweep angle, taper ratio, aspect ratio, chordwise center of gravity position, elastic axis position, pitching radius of gyration and bending-torsion frequency ratio. The original plots also include the normal values of these parameters, and their range for which these plots are valid. The plot of these two flutter indexes computed from a large number of experimental data are also shown in the original handbook[2] for delta and highly swept wings. In the computer program, only the essential data are stored and used using an automatic interpolation and data retrieval capability.

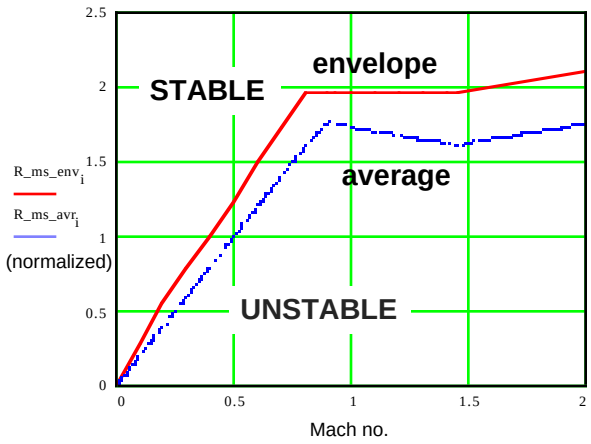

Figure 4. Flutter boundary diagram using Regier number for moderately swept wings (20<Λ<40 degrees).

Figures 4 shows the flutter boundary estimation diagram of normalized Regier number versus Mach number, for conventional planform, moderately swept wings. The first plot shows upper limits of the Regier number versus Mach number for normal values of the key basic parameters, i.e. mass ratio of 30, taper ratio of 0.6, aspect ratio of 2 and radius of gyration ratio Rgyb_60 of 0.5. The solid line is a conservative upper limit envelope and is denoted by R_ms_env(M). The lower dashed line is an average non conservative upper limit denoted by R_ms_avr(M). These two plots were compiled[2] by computing the normalized Regier number from numerous experimental data and then drawing an upper bound and a mean line through the data points. If the normalized Regier number of the wing being designed is greater than the upper bound plot over the Mach number range, then the wing is considered flutter free. If the normalized Regier number falls in between the two plots then the wing may be marginally stable. If it falls below, the wing may be unstable and would require further analysis and design.

Figures 5 shows the flutter boundary estimation diagram of the Flutter number versus Mach number, for a conventional planform, moderate sweep wing. This plot is used to estimate the equivalent flutter velocity and flutter dynamic pressure. In this figure the solid line is a conservative lower limit envelope and is denoted by F_ms_env(M). The dotted line is an average non conservative lower limit flutter boundary and is denoted by F_ms_avr(M). If the normalized Flutter number of the wing being designed is smaller than the lower bound denoted by the solid line over the Mach number range, then the wing is considered to be flutter free. If the normalized Flutter number falls in between the solid and dotted line boundaries

then the wing may be marginally stable. If the Flutter number is above the dotted line boundary, the wing may be unstable in flutter.

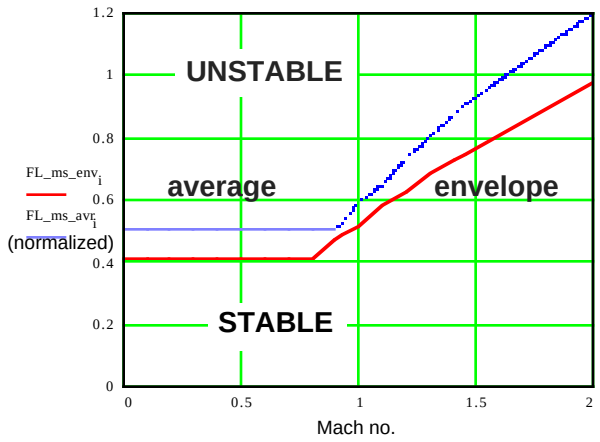

Figure 5. Flutter boundary diagram using Flutter number for moderately swept wings ($20<\Lambda<40$ degrees).

Since figures 4 and 5 are based on normalized Regier number and Flutter number, the actual Regier number and Flutter number are determined by dividing R_ms_env(M) and R_ms_avr(M) and multiplying F_ms_env(M) and F_ms_avr(M) by a total correction factor K_all, to account for actual values of the key parameters, namely mass ratio μo, taper ratio λ, aspect ratio AR, center of gravity ratio CG_R and pitch radius of gyration ratio at 60% semispan Rgyb_60. The total correction factor K_all is a product of all the key parameter correction factors for mass ratio k_μm(μo), aspect ratio K_AR(AR), CG position ratio, K_CG(CGR) and radius of gyration ratio K_Rgyb(Rgyb_60). The relationship between the key parameters and the correction factor and the plots used to determine these correction factors are presented in the appendix, to provide some insight into their effect on flutter boundary. The computer program automatically computes K_all and applies the correction factor to R_ms_env(M) and F_ms_env(M), etc. at the reference Mach number M at sea level, using the relations,

Regier_env(M) := R_ms_env(M) / K_all (6)

Flutter_env(M) := F_ms_env(M) x K_all (7)

where total correction factor K_all is defined as

K_all := K_μm(μ0) . K_Ar(AR) . K_CG(CGR) . K_Rgyb(Rgyb_60). (8)

An additional correction factor K_flex is also applied to account for wing effective root flexibility. After the correction factors are applied to the flutter boundary data from figures 4 and 5, Regier_env(M) and Flutter_env(M) are compared with surface Regier number *R* and Flutter number F of the actual wing under consideration. Thus at a given Mach number corresponding to the maximum dive speed at sea level, if the computed surface Regier number *R* and Flutter number F, satisfy the inequalities

R > Regier_env(M) (9)

F < Flutter_env(M) (10)

then the cantilever wing can be considered flutter free. On the other hand, if

Regier_env(M) > *R* > Regier_avr(M) and

Flutter_env(M) < F < Flutter_avr(M) (11)

then the wing may be marginally stable or unstable and may require redesign or refined analysis. Finally if

R < Regier_env(M) and

F > Flutter_env(M) (12)

then the wing can be considered to have unstable flutter characteristics. The computer program automatically makes these comparison, computes the flutter margins from the upper envelope and average flutter boundary, estimates flutter dynamic pressure and then plots the flutter boundary and flight dynamic pressure versus Mach number at sea level, 20000 feet and 40000 feet altitude. A summary of all the result and the flutter boundary plot as they appear in the interactive computer program are shown in Figure 6.

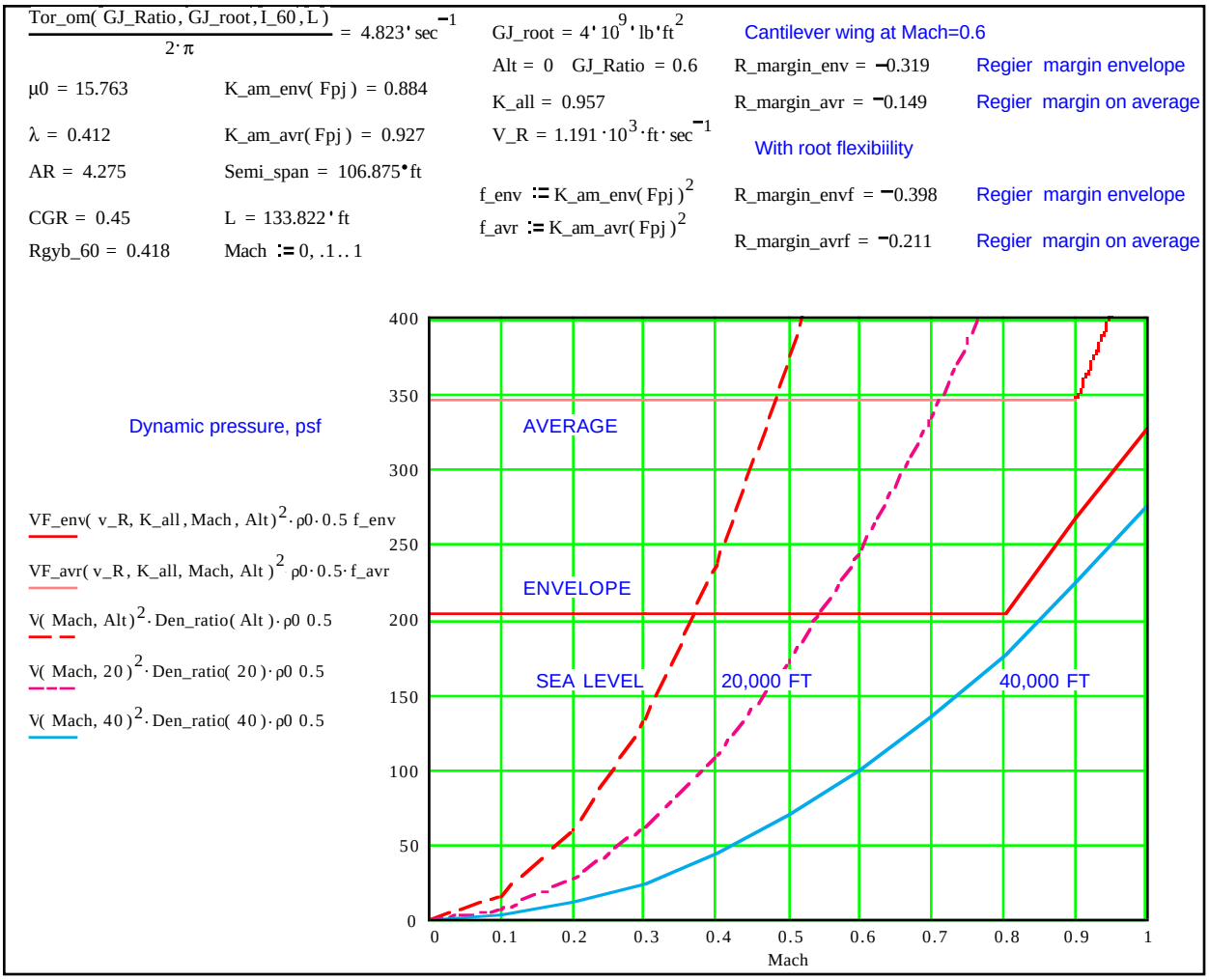

Figure 6. Summary of interactive flutter analysis result and flutter boundary plot as they appear on the computer screen.

6. Parametric Study

Figure 7 shows the geometry and structural input data used for a parametric study to determine the flutter boundary and the outer wing effective root-chord stiffness requirements of a proposed 800 passenger, 7000 nautical mile range, Blended-Wing-Body transport concept[6,7]. The outer wing has a semispan of 106.8 feet. The effective root-chord is assumed to have a torsional stiffness of 4×10^9 lb-ft^2. Using figure 3 and the method described in section 4, the torsional frequency is estimated to be 4.2 Hz. The quarter chord sweep is 37 degrees, the mass ratio is 15.8, the aspect ratio based on the outer wing semispan is 4.3, the center of gravity line is assumed to be at 45% chord, and the pitch radius of gyration ratio is assumed to be 0.42. The results presented here include an effective root flexibility correction factor K_flex between 0.88 and 0.93.

A parametric study of flutter boundary with change in effective wing-root chord torsional stiffness is presented in figures 8 and 9. This is done by assigning an array of values to the torsional stiffness variable GJ_root. The computer program automatically plots the corresponding Regier_number and Flutter_number along with the flutter boundary at the reference Mach number 0.6, at sea level as shown in these figures. The corresponding Regier velocity index and flutter velocity are also plotted in the computer program, but are not shown here.

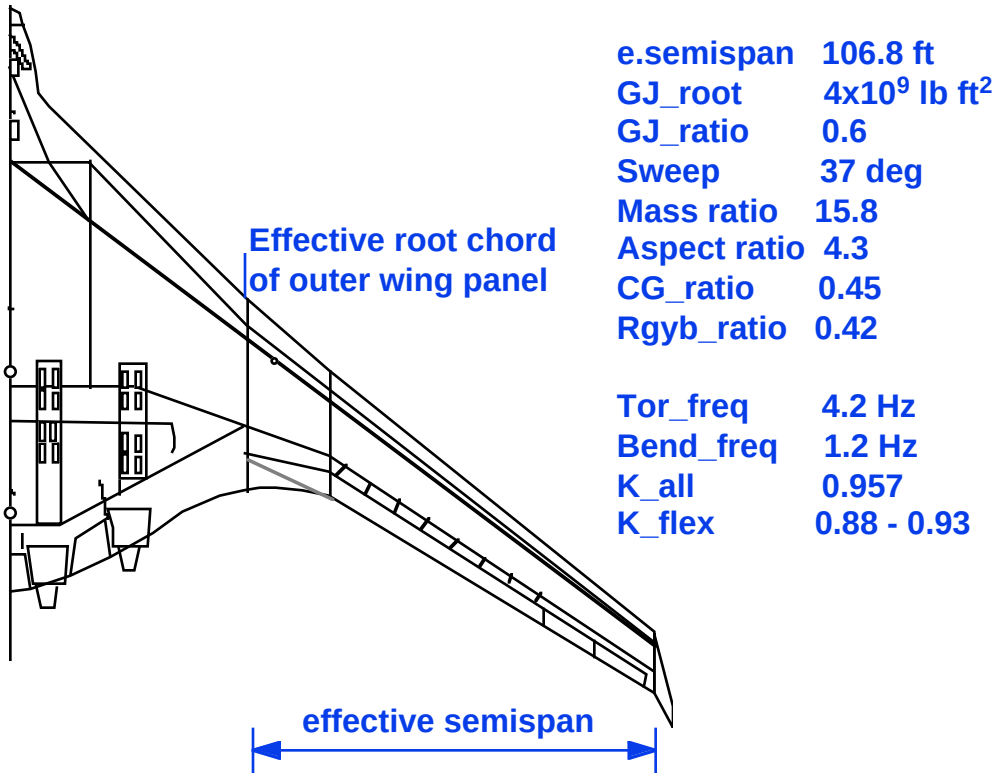

Figure 7. Geometry and structural data used for flutter analysis of the outer wing panel of the Blended Wing Body transport concept.

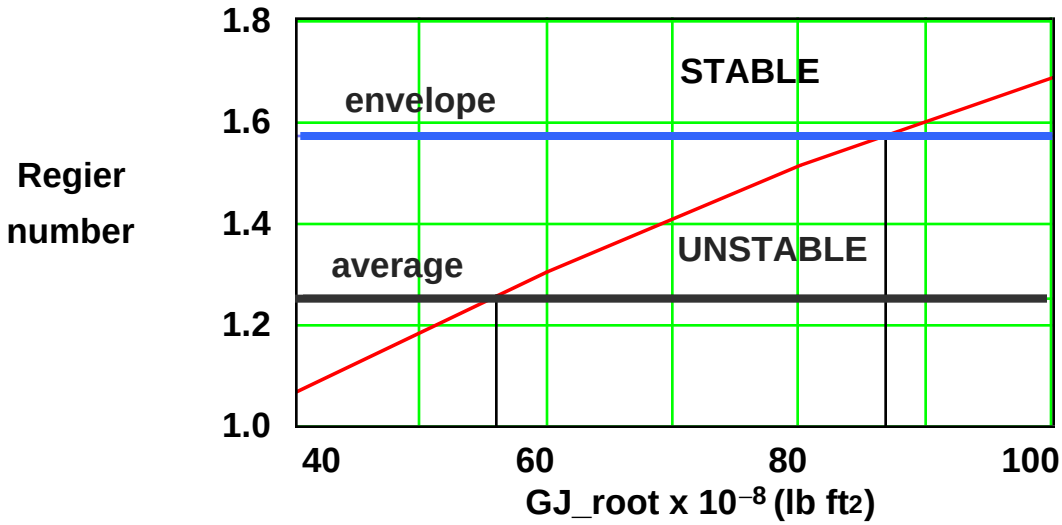

Figure 8. Variation of surface Regier number with wing root-chord torsional stiffness at a Mach no. 0.6, at sea level.

Figure 8 shows the variation of Regier number with wing root-chord torsional stiffness and the flutter boundaries at a Mach number 0.6, at sea level. The two flutter boundaries labeled 'envelope' and 'average' represent an upper boundary and a non conservative average flutter boundary, respectively[2]. If the Regier number of the wing is greater than the upper boundary of the region labeled 'stable' over the Mach number range, then the wing is considered flutter free.

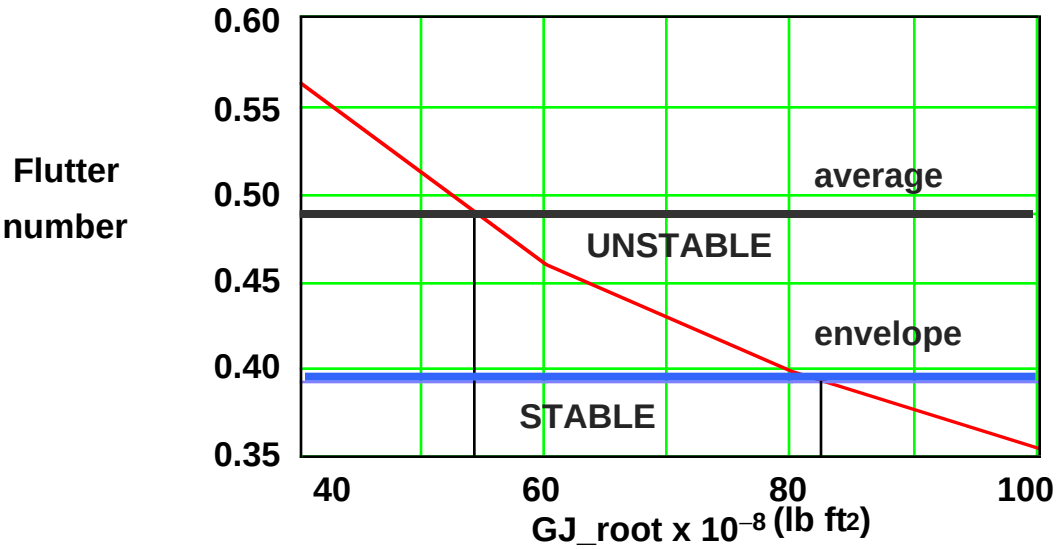

Figure 9. Plot of Flutter number vs. wing root-chord torsional stiffness at Mach no. 0.6 at sea level.

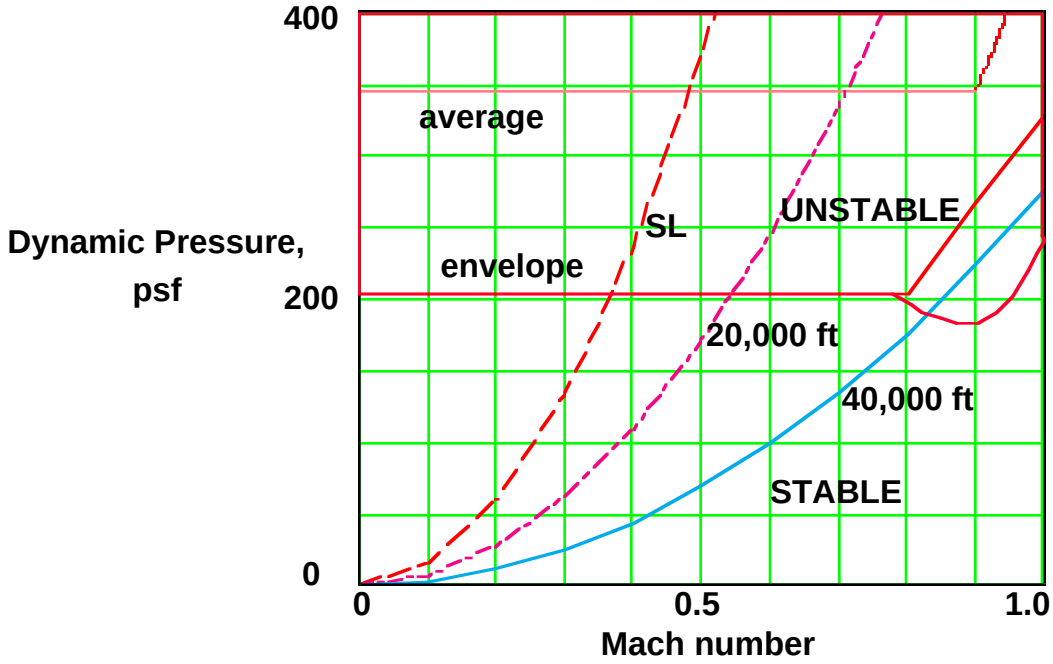

Figure 10. Outer wing flutter boundary vs. Mach number for wing-root torsional stiffness $4x10^9$ lb-ft^2.

Figure 9 shows the variation of Flutter number with wing root-chord torsional stiffness. If the Flutter number of the wing is smaller than the lower bound of the region labeled 'stable' over the Mach number range, then the wing is flutter free. Figures 8 and 9 indicate that the wing may have 20% flutter velocity margin at Mach no. 0.6 if the wing effective root-chord torsional stiffness exceeds $100x10^8$ lb-ft^2.

Figure 10 shows the initial estimates of the BWB outer wing flutter dynamic pressure boundary versus Mach number for a wing with an effective root-chord torsional stiffness of $4x10^9$ lb-ft^2, at sea level, 20000 feet and 40000 feet altitude. This figure indicates that at 40000 feet altitude, the wing would barely clear the flutter boundary at Mach 0.85. However, the wing would still be susceptible to flutter near this cruise altitude of 40000 ft and Mach number 0.85, since the

flutter dynamic pressure boundary has a dip at this transonic speed as shown in Figure 10. Hence, detailed transonic flutter analysis would be necessary and the minimum effective wing-root torsional stiffness should be much more than $4x10^9$ lb-ft^2. In these results, radius of gyration and effective wing-root flexibility effects were chosen somewhat arbitrarily and the final results are sensitive to these values. A refined flutter analysis would be required to support this preliminary analysis, if the configuration is further developed.

7. Conclusions

An easy to use, interactive computer program for rapid wing flutter analysis was developed on a MathCad platform. The analysis is based on non dimensional parametric plots of Regier number and Flutter number derived from an experimental database and handbook on flutter analysis compiled at Vought Corporation. Using this empirical method, the effects of wing torsional stiffness, sweep angle, mass ratio, aspect ratio, center of gravity location and pitch inertia radius of gyration can be easily analyzed at the conceptual design stage. The entire data and formulae used in the analysis can be displayed on computer screen in graphical and symbolic form. The analysis method was applied to investigate the flutter characteristics of the outer wing of a blended-wing-body transport concept. An Initial set of flutter instability boundaries and flutter dynamic pressure estimates were obtained. A parametric study also established that the effective wing-root chord minimal torsional stiffness should be above $100x10^9$ lb-ft^2 for a flutter free wing. In a later cycle of wing static structural design, the torsional stiffness at the effective wing-root chord station was estimated to be $200x10^9$ lb-ft^2.

APPENDIX
Correction factors

The mass ratio μo is defined as the ratio of mass of the exposed wing and mass of air at sea level in a cylinder enclosing the semispan with semichord as its radius.

$$\mu 0 = \frac{W\_ex}{\pi \cdot \rho 0 \cdot \int_0^S b^2 \, dy}$$

The correction factor K_µms plot for a medium sweep wing is shown in figure 11 for nominal mass ratio of 30. The plot indicates that increased mass ratio decreases flutter stability margin since, a lower correction factor decreases the flutter boundary envelope Flutter_env(M) as indicated in Eq.(7). The physical reason is that the increased mass ratio represents reduction in torsional frequency and increased aerodynamic force.

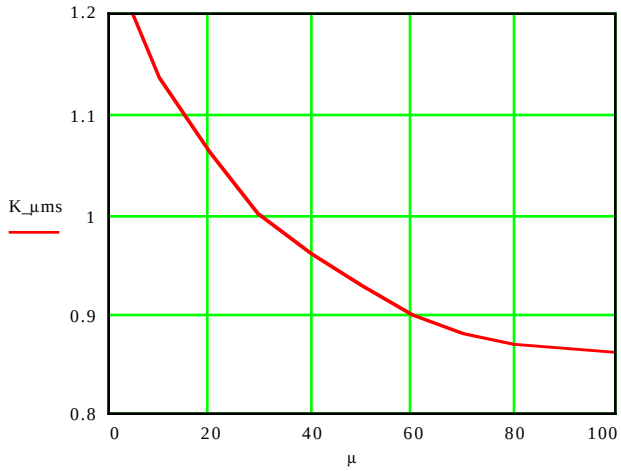

Figure 11. Mass ratio correction factor K_µms for medium sweep wing.

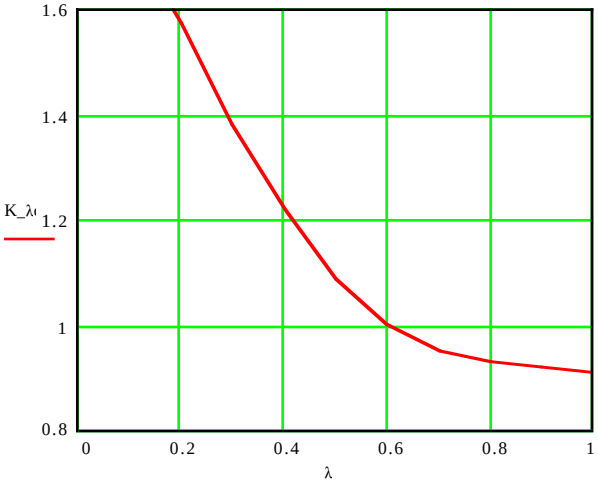

Figure 12 Taper ratio correction factor K_λ.

The plot for determining the correction factor K_λ for taper ratio is shown in figure 12, which indicates that increased taper ratio would decrease flutter stability margin in general, due to decreased Flutter_env(M) as indicated by Eq.(7). The reduction in margin is more pronounced for taper ratios less that 0.6. Physically this is due to increased wing outboard flexibility

The plot for determining the correction factor K_Ar for aspect ratio is shown in figure 13, which indicates

that increased aspect ratio would decrease flutter stability margin.

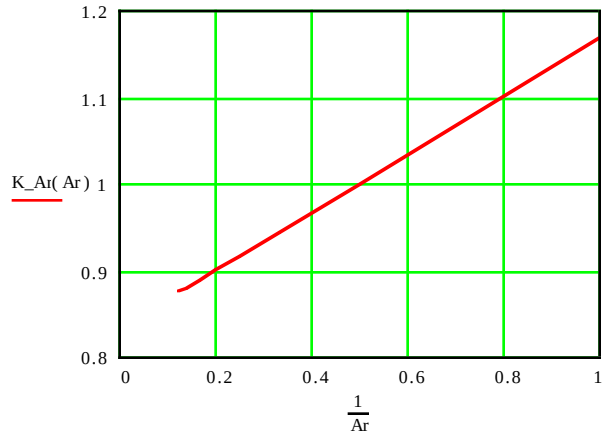

Figure 13 Aspect ratio correction factor K_Ar.

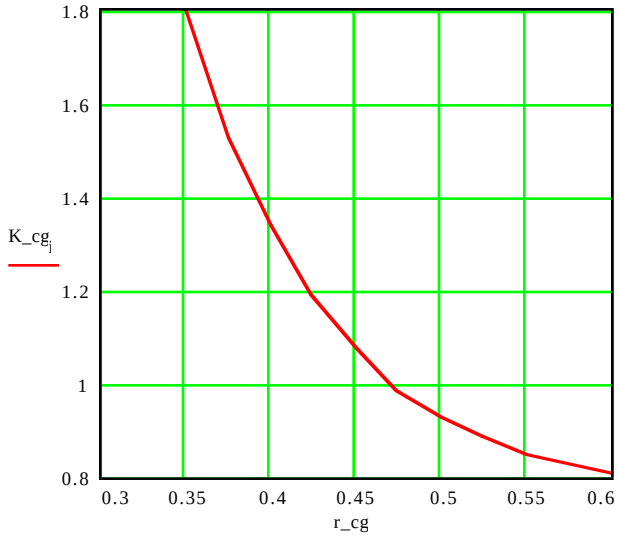

Figure 14 Center of gravity correction factor K_cg.

The plot for determining the correction factor K_cg for chordwise position of center of gravity is shown in figure 14, which indicates that rearward movement of CG would decrease flutter stability, due to reduced pitch inertia. The wing mounted engines have forward overhang to move the overall CG forward. The radius of gyration ratio at 60% semispan is defined by

$$Rgyb\_60 := \frac{1}{b} \cdot \sqrt{\frac{I\_60}{W\_60}}$$

Figure 15 shows the plot for determining correction factor K_Rgyb for nominal value of 0.5 for Rgyb. This figure indicates that increased radius of gyration has beneficial effect on flutter stability margin, due to increased pitch inertia.

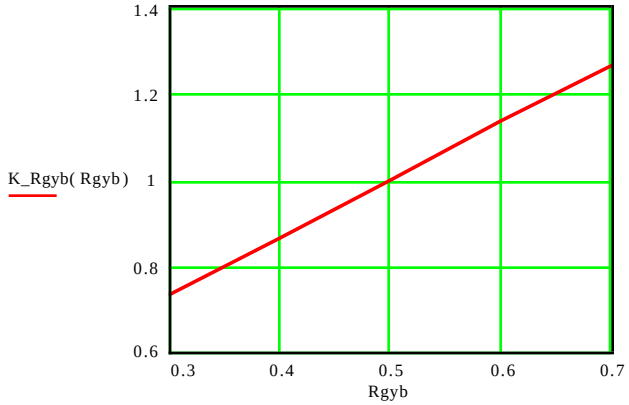

Figure 15 Radius of gyration ratio correction factor K_Rgyb.

References

1. MathCad, Version.3.1 Users Guide, MathSoft Inc., 201 Broadway, Cambridge, Mass 02139, 1991.

2. Harris, G., "Flutter Criteria for Preliminary Design," LTV Aerospace Corporation., Vought Aeronautics and Missiles Division, Engineering Report 2-53450/3R-467 under Bureau of Naval Weapons Contract NOW 61-1072C, September 1963.

3. Regier, Arthur A., "The Use of Scaled Dynamic Models in Several Aerospace Vehicle Studies, "*ASME Colloquium on the Use of Models and Scaling in Simulation of Shock and Vibration*, November 19, 1963, Philadelphia, PA.

4. Frueh, Frank J., "A Flutter Design Parameter to Supplement the Regier Number," AIAA Journal. Vol. 2, No. 7, July 1964.

5. Dunn, Henry J. and Doggett, Robert V. Jr., "The Use of Regier Number in the Structural Design with Flutter Constraints," NASA TM 109128, August 1994.

6. Liebeck, Robert, H., Page, Mark, A., Rawdon, Blaine K., Scott, Paul W., and Wright Robert A., "Concepts for Advanced Subsonic Transports," NASA CR-4628, McDonnell Douglas Corporation, Long Beach, CA, September 1994.

7. Sweetman Bill and Brown Stuart F, "Megaplanes, the new 800 passenger Jetliners," Popular Mechanics, April 1995, pp. 54-57.